Aalborg Universitet

AALBORG UNIVERSITY
DENMARK

Optics of multiple grooves in metal

Transition from high scattering to strong absorption

Skjølstrup, Enok Johannes Haahr; Søndergaard, Thomas; Pedersen, Kjeld; Pedersen, Thomas Garm

Link to publication from Aalborg University

PROCEEDINGS OF SPIE

Optics of multiple grooves in metal: transition from high scattering to strong absorption

Enok J. H. Skjølstrup, Thomas Søndergaard, Kjeld Pedersen, Thomas G. Pedersen

SPIE.

Optics of multiple grooves in metal: transition from high scattering to strong absorption

Enok J.H Skjølstrup[a], Thomas Søndergaard[a], Kjeld Pedersen[a], and Thomas G. Pedersen[a]

[a]Department of Materials and Production, Aalborg University, Skjernvej 4A, DK-9220 Aalborg East, Denmark

ABSTRACT

This paper studies theoretically how the optics of multiple grooves in a metal change as the number of grooves is increased gradually from a single groove to infinitely many arranged in a periodic array. In the case of a single groove the out-of-plane scattering (OUP) cross section at resonance can significantly exceed the groove width. On the other hand a periodic array of identical grooves behaves radically different and is a near-perfect absorber at the same wavelength. When illuminating multiple grooves with a plane wave the OUP cross section is found to scale roughly linearly with the number of grooves and is comparable to the physical array width even for widths of many wavelengths. The normalized OUP cross section per groove even exceeds that of a single groove, which is explained as a consequence of surface plasmon polaritons generated at one groove being scattered out-of-the-plane by other grooves. In the case of illuminating instead with a Gaussian beam, and observing the limit as the incident beam narrows and is confined within the multiple-groove array, it is found that the total reflectance becomes very low and that there is practically no out-of-plane scattering. The well-known result for periodic arrays is thus recovered. All calculations were carried out using Greens function surface integral equation methods taking advantage of the periodic nature of the structures. Both rectangular and tapered grooves are considered.

Keywords: Surface plasmons, diffraction and gratings, scattering theory, metal optics

1. INTRODUCTION

Optics of grooves in metal have attracted attention due to their interesting scattering and absorption properties. The optical cross sections of a single sub-wavelength ultrasharp or tapered groove in metal has been theoretically studied in detail in[1] establishing several fundamental results describing how the cross sections depend on the groove dimension. Here it was found that the out-of-plane scattering cross section can exceed the physical width of the groove in a broad wavelength interval. For a rectangular and tapered groove instead, the cross sections are found to be significantly large only for a narrow band of wavelengths.[2–4] A periodic array of ultrasharp grooves is on the other hand found to give rise to broadband absorption, thus turning a shiny, highly reflecting surface into a black surface.[5, 6] Thus a single groove and multiple grooves behave quite different, and in[1] it was suggested that the very low reflectance of the periodic array was due to mutual destructive interference between the scattered fields from the individual grooves. This hypothesis was recently tested in[7] where the optics of multiple ultrasharp grooves in metal was studied as the transition from one to infinitely many grooves. Surprisingly, it was found that the hypothesis was not correct when the incident field is a plane wave. The OUP cross section was found to scale approximately linear with the number of grooves and to be approximately 1.5 times larger than the physical width of the grooves even for widths of many wavelength. Instead it was found that when illuminating 20 grooves with a Gaussian beam entirely focused within the grooves, the reflectance is the same as for a periodic array illuminated by a plane wave. In this paper we explore the same transition as in[7] but for rectangular and tapered (not ultrasharp) grooves and show that the same principles apply for these types of grooves when they are combined in an array of multiple grooves.

An application for arrays of tapered grooves in metal is to use them in constructing broadband omnidirectional absorbers and angularly selective emitters.[8] As only p-polarized light will be efficiently absorbed in the grooves,

---

while s-polarized light will be almost perfectly reflected, an array of ultrasharp grooves can be applied as polarizers for ultrashort laser pulses.[9] As the rectangular and tapered grooves only absorb light for wavelengths close to the resonance, an application for those grooves is in selective thermal emitters[10,11] which can be advantageous in thermophotovoltaics.[12,13]

The structure of interest in this paper is illustrated in Fig. 1(c), where the grooves can be either rectangular (Fig. 1(a)) or tapered (Fig. 1(b)). The rectangular grooves have a depth of 500 nm and a width of 50 nm while the tapered grooves have a depth of 350 nm, a top width of 100 nm, and a bottom width of 60 nm, where all the corners are rounded by a circle with radius of 4 nm as in[2] implying that the top width of the rectangular grooves is 58 nm. The incident field in Fig. 1(c) is a normal Gaussian beam with beam waist radius w_0 centered at $x = x_0$ in the middle of the array of N identical grooves. There is a distance d between the grooves and the total length of the groove array is denoted L. The beam waist radius is related to the array length by $w_0 = \gamma L/2$, where γ is a ratio parameter determining the width of the Gaussian beam, and $\gamma = 1$ has been applied in illustrating Fig. 1(c). The incident light can be either reflected or scattered upwards, absorbed in the metal, or scattered into surface plasmon polaritons (SPPs) which are electromagnetic waves bounded to and propagating along the metal surface. As in[7] the magnetic field only has a z-component ($\mathbf{H}(\mathbf{r}) = \hat{z}H(\mathbf{r}) = \hat{z}H(x,y)$) and the structure
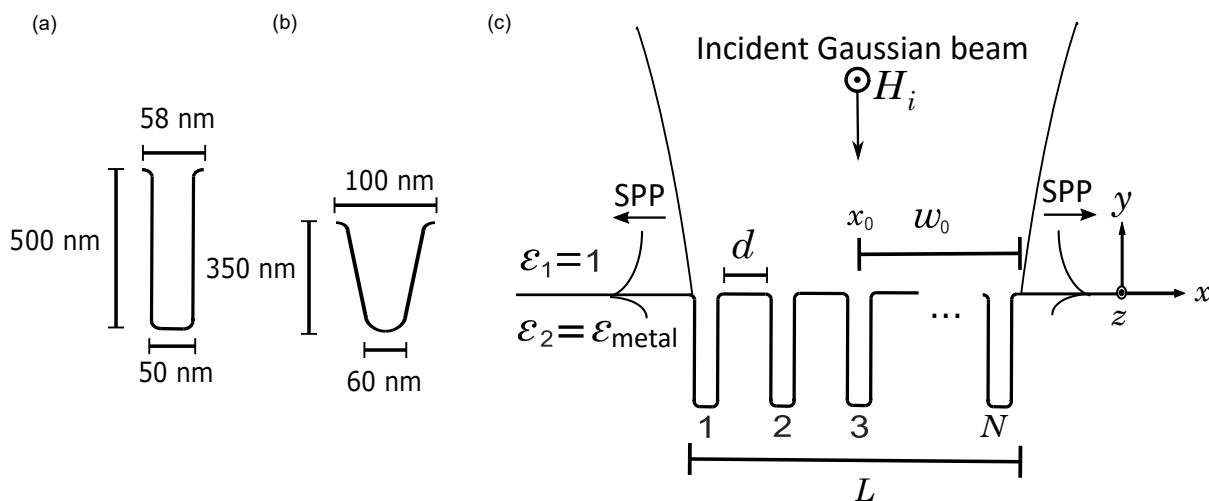

Figure 1. Schematic of N identical rectangular grooves in metal separated by the distance d. The incident field is a normal Gaussian beam with beam waist radius w_0 centered in the middle of the groove array ($x = x_0$).

is considered invariant in the z-direction, which implies that 2D-calculations are performed. Gold is applied as the metal and the dielectric constant of gold is from.[14] The calculations are performed using the Greens function surface integral equation method (GFSIEM) as presented in appendix B in.[2] See[7] for a further description of how the matrix equation is constructed and solved using the iterative method GMRES.[15,16]

The paper is organized in the following way. Section 2 contains the case with a plane wave ($w_0 = \infty$) as the incident field, and here extinction, scattering, and absorption cross sections are calculated for a structure of varying N where the grooves are rectangular with the aforementioned dimensions. A Gaussian beam is used as the incident field in Section 3 where the grooves are still rectangular. Here the beam waist radius is varied, and angular reflection spectra and total out-of-plane reflected power is calculated. In Section 4 the grooves are tapered, and here both optical cross sections and reflectance as a function of wavelength is presented.

2. PLANE WAVE AS INCIDENT FIELD

In this section the incident field is a plane wave, which means that the beam waist radius w_0 in Fig. 1(c) tends to infinity. When light is incident on the multiple grooves, scattering occurs and some light is coupled into SPPs propagating along the metal surface away from the grooves, some light is scattered out of the plane, and some

light is absorbed in the metal. Extinction (EXT) refers to the amount of power removed from the reflected beam due to scattering and absorption. The corresponding EXT, OUP, and SPP cross sections are obtained by normalizing the respective powers by the power per unit area of the incident light. The absorption (ABS) cross section is given by the EXT cross section minus the OUP and SPP cross sections. See appendix B in[2] for a description of how the cross sections are calculated using the GFSIEM.

The rectangular shape of the grooves is found to give rise to a narrowband resonant behaviour in all the cross sections.[2] For the particular dimensions of the grooves considered here, the cross sections of a single groove are found to be resonant at a wavelength of 660 nm as seen in Fig. 5(a). Before multiple grooves are considered it is chosen to study cross sections for a structure of only two grooves depending on the distance between them. It is chosen to fix the wavelength at $\lambda_0 =660$ nm, and the EXT, OUP, and SPP cross sections are seen in Fig. 2 as a function of distance between the two grooves. All the cross sections are oscillating with certain extreme values to
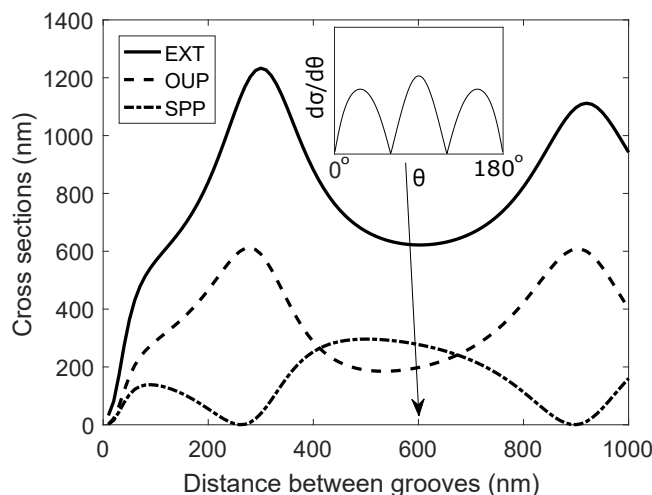

Figure 2. EXT, OUP, and SPP cross sections for a structure of 2 grooves with varying distance d between the grooves. The inset shows the differential OUP cross section at $d = 600$ nm. The wavelength is 660 nm.

be explained. For the SPP cross section the first minimum is found at $d =260$ nm. With a top width of a single groove at 58 nm (see Fig. 1(a)), the period of the structure for this d is 318 nm, which equals a half plasmon wavelength, where $\lambda_{SPP} = \sqrt{(\epsilon_1 + \epsilon_2')/\epsilon_1\epsilon_2'}\lambda_0 = 635$ nm where ϵ_2' is the real part of ϵ_2.[17] Hence at $d = 260$ nm the SPPs generated at the different grooves interfere destructively implying that the SPP cross section is practically 0. When this happens much of the light is instead coupled out of the plane, as seen by the fact that the OUP cross section is a maximum at almost the same d as SPP is minimized. When d increases towards a plasmon wavelength, plasmons generated at the different grooves interfere constructively implying that SPP has a maximum, and at approximately the same d both the OUP and EXT have a minimum. At $d = 300$ nm the EXT cross section has a maximum, and at $d = 600$ nm it has a mimimuim, and therefore it is chosen to consider these distances in the following. The inset in Fig. 2 shows the differential OUP cross section for $d = 600$ nm. Here interference similar to a double slit predicts that destructive interference occurs at 60 and 120°, which is verified in the inset.[18]

For multiple grooves the EXT, OUP, and ABS cross sections are seen at a wavelength of 660 nm in Fig. 3 when the distance d is 300 nm in (a) and 600 nm in (b). Especially in Fig. 3(a) the cross sections are almost linear functions of the number of grooves, while in Fig. 3(b) the linear behaviour first begins after approximately 10 grooves. It is clearly seen that the cross sections in Fig. 3(a) are much larger than those in Fig. 3(b), and this large difference is not entirely caused by the fact that the EXT and OUP cross sections are smaller for $d = 600$ nm than for $d = 300$ nm according to Fig. 2. As will be shown in Fig. 5(b) for $d = 600$ nm the resonance wavelength is blue-shifted from the 660 nm being the resonance wavelength of a single groove and, furthermore a smaller peak occurs around 700 nm. Hence, when the wavelength is 660 nm as is the case in Fig. 3 there is no resonance for $d = 600$ nm which implies that the cross sections are much smaller compared to Fig. 3(a). For
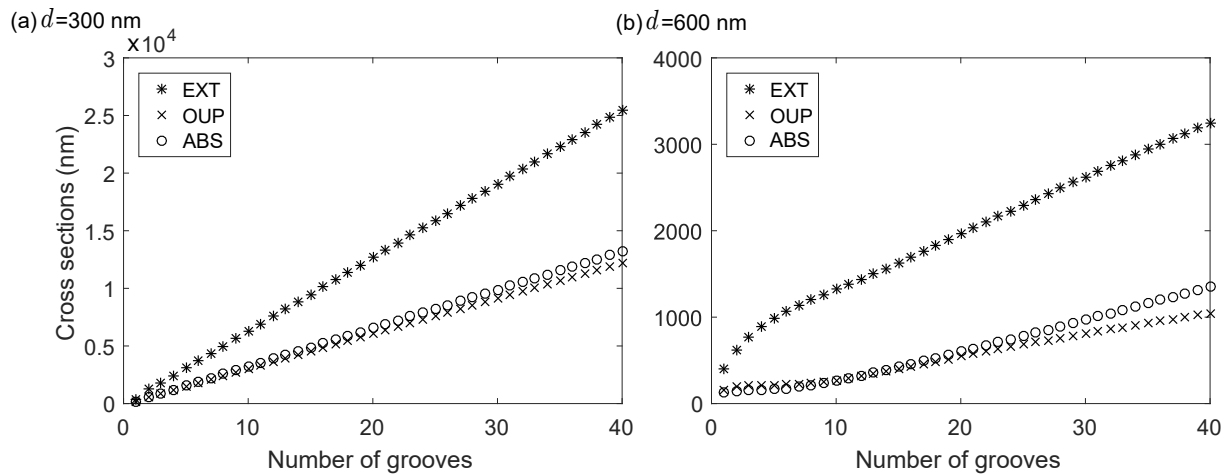
Figure 3. EXT, OUP, and ABS cross sections at $\lambda = 660$ nm, where $d = 300$ nm in (a) and $d = 600$ nm in (b).

$N = 40$ grooves the OUP cross section is approximately 12 μm for $d = 300$ nm, and here the total length of the groove array is $L \approx 14\mu$m. However, the grooves themselves only occupy approximately 1/6 of the length, as the distance d between the grooves is much larger than the groove width. The OUP cross section per groove is seen in Fig. 4 where again $d = 300$ nm in (a) and $d = 600$ nm in (b). In Fig. 4(a) the OUP per groove converges to approximately 300 nm which is approximately 0.85 times the groove period, but more than 5 times larger than a single groove width. For $d = 600$ nm the OUP cross section for 40 grooves is approximately 1μm as seen in Fig. 3(b), and the OUP per groove thus converges to approximately 25 nm as seen in Fig. 4(b). This much smaller cross section per groove is again due to the fact that for $d = 600$ the wavelength at 660 nm is not resonant.
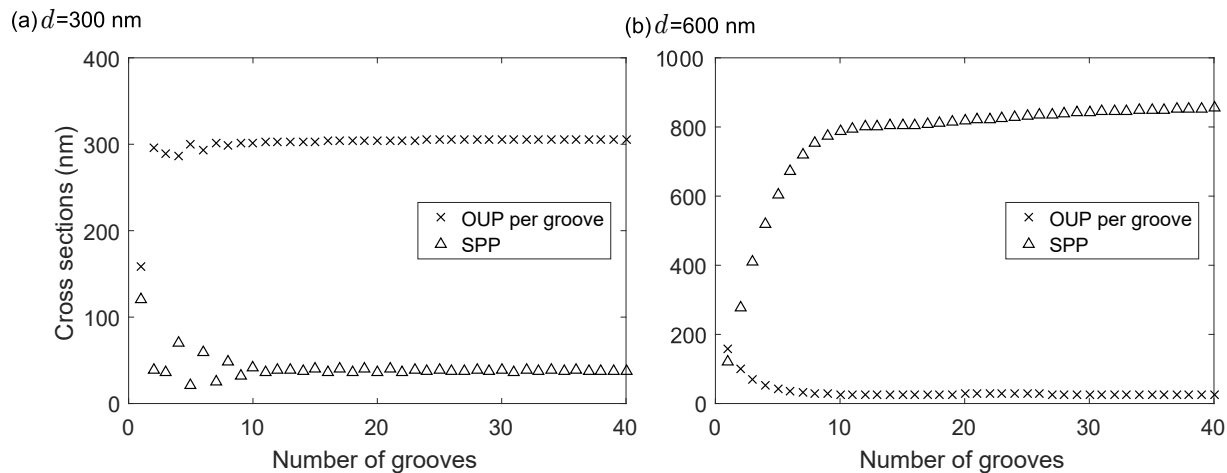
Figure 4. SPP and OUP cross sections per groove at $\lambda = 660$ nm, where $d = 300$ nm in (a) and $d = 600$ nm in (b)

The linear behaviour of the EXT, OUP, and ABS cross section as a function of number of grooves was recently found for ultrasharp grooves in,[7] where the OUP per groove was found to be approximately 1.5 times the groove period. In that study the grooves had a wide opening at 240 nm in the top and a bottom width of only 0.3

nm with only $d = 10$ nm between the grooves. Furthermore, the reflectance of an infinite array of the same grooves illuminated by a plane wave was found in[5] to be 16% for this particular wavelength at 770 nm, and the extraordinary large OUP cross section for a structure consisting of 40 grooves was therefore a surprising and remarkable result. For the rectangular grooves considered in this paper the OUP cross section per groove is thus comparable to,[7] but with the difference that it is smaller than the groove period (by the factor ≈ 0.85) but much larger than a single groove width (by the factor > 5).

The SPP cross section is shown by the triangles in Fig. 4 being a damped oscillatory function in Fig. 4(a) and an increasing function in Fig. 4(b). According to Fig. 2 the distance $d = 300$ nm is close to the minimum where the plasmons generated at different grooves interfere destructively resulting in a small SPP cross section. Another phenomena which implies a small SPP cross section is the fact that a plasmon generated at one groove can be coupled out of the plane by another groove as examined in.[19–21] In[7] this effect was studied in more detail and was found to be a contributing cause to the out of plane scattering when the structure consists of multiple grooves. In Fig. 4(b) the distance d is close to the maximum of SPP cross section according to Fig. 2. Here plasmons generated at different grooves interfere constructively resulting in an overall increase of the total SPP cross section. Hence if the purpose of the structure is to efficiently excite plasmons the groove period should be close to the plasmon wavelength as studied in.[22,23] In addition it was found in[24,25] that the dimensions of the individual grooves can be optimized in such a way that most of the incident light is excited into SPPs.

While only a wavelength of 660 nm has been considered so far, the EXT cross section is seen as a function of wavelength for a structure consisting of 1, 5, 10, and 20 grooves in Fig. 5 for $d = 300$ nm in (a) and $d = 600$ nm in (b). Especially in Fig. 5(a) the EXT cross section scales approximately linear with N for
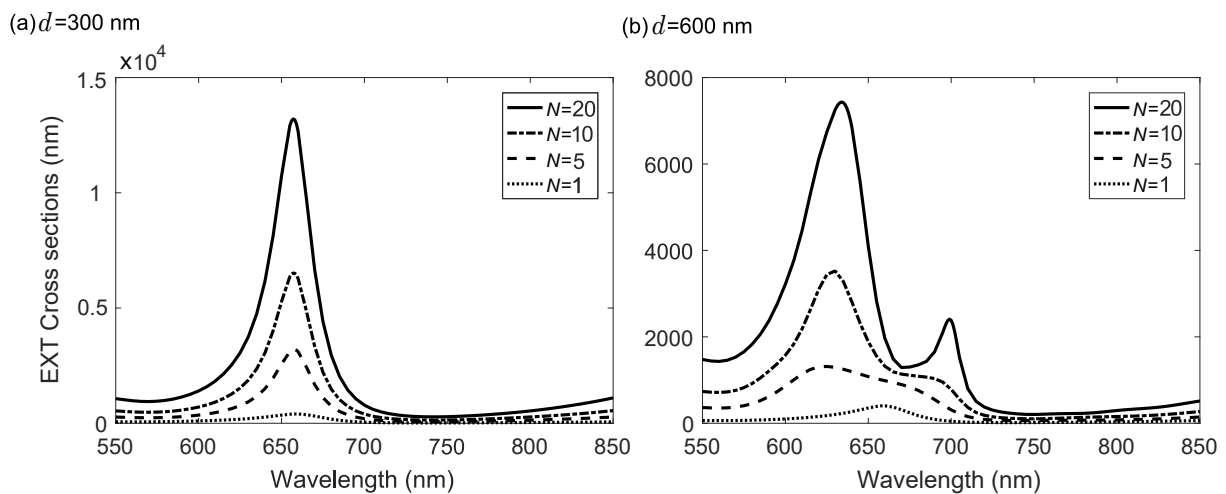

Figure 5. EXT cross sections for 1, 5, 10, and 20 grooves as a function of wavelength, where $d = 300$ nm in (a) and $d = 600$ nm in (b).

all considered wavelengths, and the same is found for the OUP and ABS cross sections (not shown). Here the resonance wavelength has slightly changed from 660 nm for one groove into 657 nm for 20 grooves. This change in resonance wavelength is more pronounced in Fig. 5(b) where it is blue-shifted by approximately 30 nm compared to the spectrum for a single groove, but as N increases the resonance wavelength slightly red-shifts again. As in Fig. 5(a) the EXT cross section scales roughly linear with N at most wavelengths. However, in Fig. 5(b) the groove period is comparable to the wavelength, which implies that Rayleigh-Wood anomalies splits the resonance wavelength into two peaks instead of one.[26–28] This splitting is more pronounced for $N = 20$ implying that the linear scaling of EXT with N fails for wavelengths around 700 nm for $N < 20$.

The same linear scaling of EXT cross section for many wavelengths was recently found in[7] for ultrasharp grooves, where the cross sections were large in a much broader wavelength interval. Based on this linear scaling for a specific groove dimension and the study of the cross sections of a single groove for many different groove

dimensions in[1] it was postulated in[7] that the linear scaling will also be valid for other groove dimensions, and Fig. 5(a) seems to confirm this for a rectangular groove being a narrowband resonator.

As seen in Fig. 3 the OUP cross section scales approximately linear with the number of grooves. To further study the out of plane scattering from multiple grooves the differential OUP cross section is shown in Fig. 6 for a structure consisting of 1, 5, 10, and 20 grooves with $d = 300$ nm and $\lambda = 660$nm. The differential cross sections have all been normalized such that they have a maximum of 1. When many grooves are present the angular distribution clearly becomes much more narrow. Notice that the OUP cross section is found by integrating the differential OUP cross section from 0-180°.
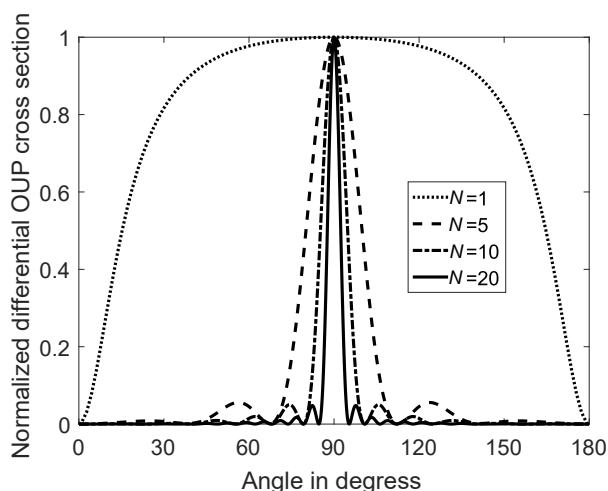

Figure 6. Normalized differential OUP cross sections for 1, 5, 10, and 20 grooves for $\lambda = 660$ nm and $d = 300$ nm.

3. GAUSSIAN BEAM AS INCIDENT FIELD

In this section the incident field is a Gaussian beam with beam waist radius $w_0 = \gamma L/2$ as illustrated in Fig. 1(c) for $\gamma = 1$. The same type of calculations as in[7] are performed, see e.g the appendix in[7] for a further explanation of the relevant terms.

First it is studied how the incident field and reflected field depend on the ratio parameter γ which determines the width of the Gaussian beam. A structure consisting of 20 grooves with $d = 300$ nm between the grooves is considered and the wavelength is chosen to be 660 nm. The incident power per angle is seen by the bright lines (blue online) in Fig. 7 for $\gamma = 0.5$ and 2 and even for such small γ the beam is still paraxial (meaning that $2\pi w_0/\lambda >> 1$) as the structure has been chosen to be sufficiently wide such that this is achived for $\gamma \geq 0.5$. It is clearly seen that a smaller γ implies that the angular distribution is broader. The reflected power per angle is seen in black in the same figure when $\gamma = 0.5$, 2, and 100. For $\gamma = 100$ the incident field is so wide that it mostly hits the planar surface surrounding the grooves and the grooves themselves only marginally contribute. Therefore the incident and reflected beams are almost the same, why only the reflected field is shown in Fig. 7, and it is very narrow in angular distribution as it behaves almost like a plane wave. The reflectance is found as the area under the black curve divided by the area under the corresponding blue curve and is found to be 0.03, 0.31, and 0.95 when $\gamma = 0.5$, 2, and 100, respectively. Hence the reflectance strongly depends on γ since a high γ implies that the Gaussian beam also hits the planer surface and not entirely the grooves. This is found not to be the case for $\gamma \leq 0.5$ why in this case the calculated reflectance is entirely due to the grooves and not the surrounding planar surface.

The reflectance is thus calculated as a function of γ and is shown by the asterisks in Fig. 8(a) for the same structure consisting of 20 grooves with $d = 300$ nm, notice that the γ-axis in the figure is on a log scale. As mentioned in Sec. 2 the resonance wavelength for the structure consisting of 20 grooves has slightly changed
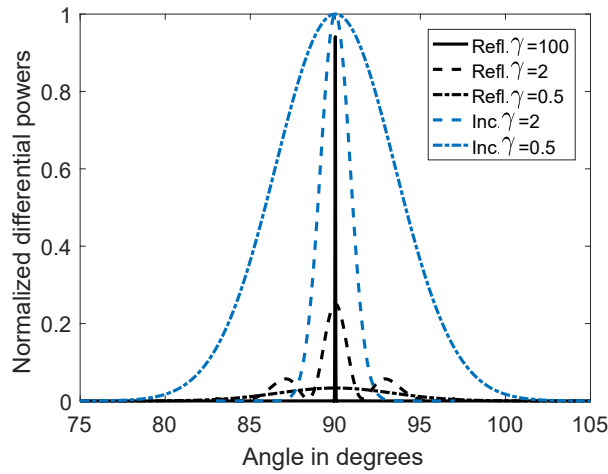
Figure 7. Normalized differential incident power for varying γ is seen by the bright lines (blue online) and the normalized differential reflected power in black. The wavelength is $\lambda = 660$ nm and $d = 300$ nm.
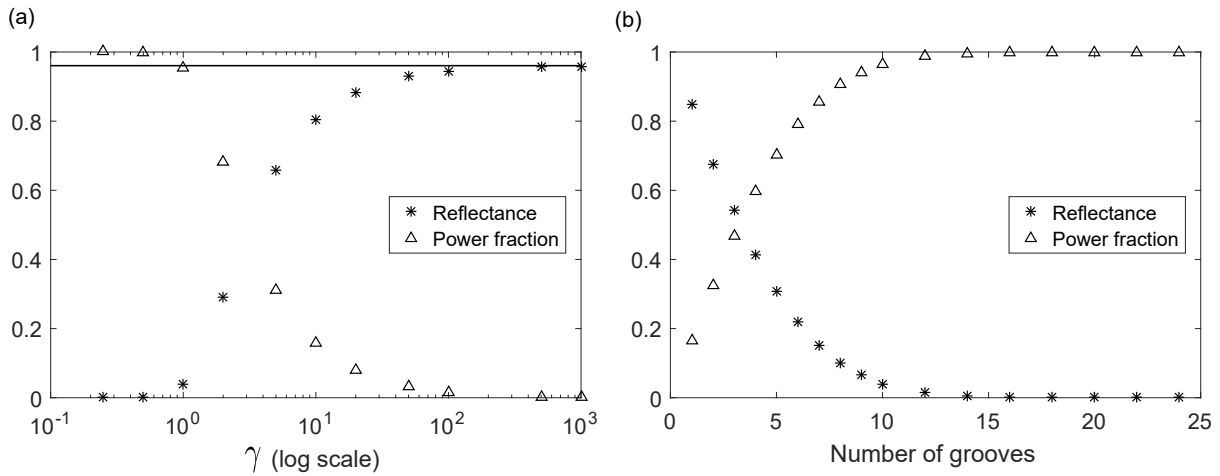

Figure 8. (a) Reflectance and power fraction as a function of γ for 20 grooves with $d = 300$ nm. (b) Reflectance and power fraction as a function of number of grooves for a fixed beam waist $w_0 = 1715$ nm. The wavelength is 657 nm in both (a) and (b).

into 657 nm, why this wavelength has been used in Fig. 8(a) while 660 nm was the wavelength in Fig. 7. The reflectance is seen to converge for both small and large γ, where it converges to the proper reflectance which is entirely due to the grooves when $\gamma \leq 0.5$ and converges to that of a flat gold surface when γ is large, as illustrated by the black horizontal line in the figure. The power fraction illustrated by the triangles in the same figure show the geometric fraction of the incident power that actually hits the grooves. This fraction is practically 1 for $\gamma \leq 0.5$ and is practically 0 for $\gamma \geq 500$. Importantly notice that the reflectance and power fraction converge for the same γ

3.1 Reflectance as a function of number of grooves

In this subsection it is studied how the reflectance depends on the number of grooves for a fixed beam waist radius w_0 which is set to 1715 nm corresponding to $\gamma = 0.5$ for 20 grooves. In Fig. 8(b) the reflectance as a

function of number of grooves is seen for $\lambda = 657$ nm and converges to practically 0 when 20 grooves are present. Thus it is found that 20 grooves are sufficient to obtain the same reflectance as a structure consisting of infinitely many grooves. As in Fig. 8(a) the triangles show the power fraction and it converges to 1 when 20 grooves are present as was also observed in Fig. 8(a). Hence Fig. 8 shows that the reflectance converges to the proper reflectance of the grooves when all the incident light hits the groove array. The same result was obtained in[7] for ultrasharp grooves.

While Fig. 8 only considered $\lambda = 657$ nm the reflectance as a function of wavelength is seen in Fig. 9 for 5 to 20 grooves, where again $d = 300$ nm in (a) and $d = 600$ nm in (b). It is clearly seen that the reflectance at
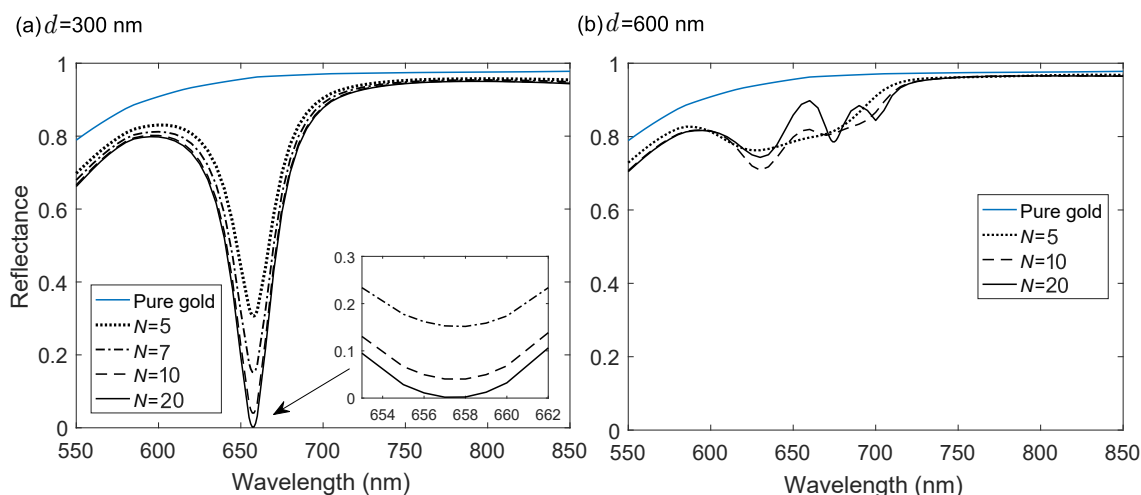

Figure 9. Reflectance as a function of wavelength for 5 to 20 grooves, where $d = 300$ nm in (a) and $d = 600$ nm in (b). Inset in (a) shows the reflectance in a smaller wavelength interval.

resonance is much lower for $d = 300$ nm than for $d = 600$ nm. From Fig. 5 the EXT cross sections was found to be roughly 1.5 times larger for $d = 300$ nm than for $d = 600$ nm, and this relatively small factor can not itself be responsible for the much higher reflectance for $d = 600$ nm in Fig. 9(b). When $d = 600$ nm the grooves themselves only occupy approximately $1/11$ of the total array length L, and the most of the array is thus pure gold which explains why the reflectance in Fig. 9(b) is relatively close to that of pure gold even when 20 grooves are present. In Fig. 9(a) the reflectance is shown for 5, 7, 10, and 20 grooves, and here the reflectance is low close to the resonance wavelength and comparable to that of pure gold for longer wavelengths. Here more grooves imply that the reflectance at resonance becomes lower as was also observed in Fig. 8(b) but off resonance the reflectance is almost independent on the number of grooves. The inset in Fig. 9(a) shows the reflectance for a smaller wavelength interval close to the resonance wavelength, and here it is possible to see the difference in reflectance between 10 and 20 grooves. It is remarkable that the reflectance of 20 grooves when illuminating with a Gaussian beam becomes practically 0 when the same groove structure illuminated with a plane wave has a very large OUP cross section as observed in Sec. 2. The same kind of result was found in[7] for ultrasharp grooves and there it was postulated to be valid for other groove dimensions as well, and Fig. 9(a) confirms this for rectangular grooves.

3.2 Energy Transportation

As in[7] the energy transportation is investigated based on the time-averaged Poynting vector $\langle \mathbf{S} \rangle = 1/2 \mathrm{Re} \left(\mathbf{E} \times \mathbf{H}^* \right)$ where $\mathbf{E}$ and $\mathbf{H}$ are the complex electric and magnetic field, respectively, and where * denotes complex conjugation. The interpretation of the Poynting vector is that it points in the direction of the power flow with a magnitude describing the power flow per unit area.[17] Fig. 10 illustrates the magnitude of the time-averaged Poynting vector when a Gaussian beam with ratios of 0.5, 1, 2, and ∞ (plane wave) is incident on a structure consisting of 20 grooves with $d = 300$ nm between the grooves and with a wavelength of 660 nm. The black

horizontal lines in the figure illustrate the length of the groove array. Both the reference field and the scattered field have been included in the calculation of the Poynting vector. When $\gamma = 0.5$ the incident field is entirely focused within the grooves (see Fig. 8(a)) which implies that there is almost no light scattered out of the plane. This is clearly observed in Fig. 10(a) where the magnitude of the Poynting vector is zero for all other positions than right above the groove array. When γ increases more light is scattered out of the plane as observed in Fig. 10(b)-10(d). When the incident field is a plane wave as in Fig. 10(d) most of the incident light hits the planar surface surrounding the grooves where they experience almost total reflectance as pure gold is almost a perfect mirror at this wavelength. Hence far outside the grooves the net power flow is very low. The angular distribution of the scattered field is broader for $\gamma = \infty$ than for $\gamma = 2$ (Fig. 10(c)) which was also partly observed in Fig. 7 as the oscillations in differential powers for angles deviating from 90°.
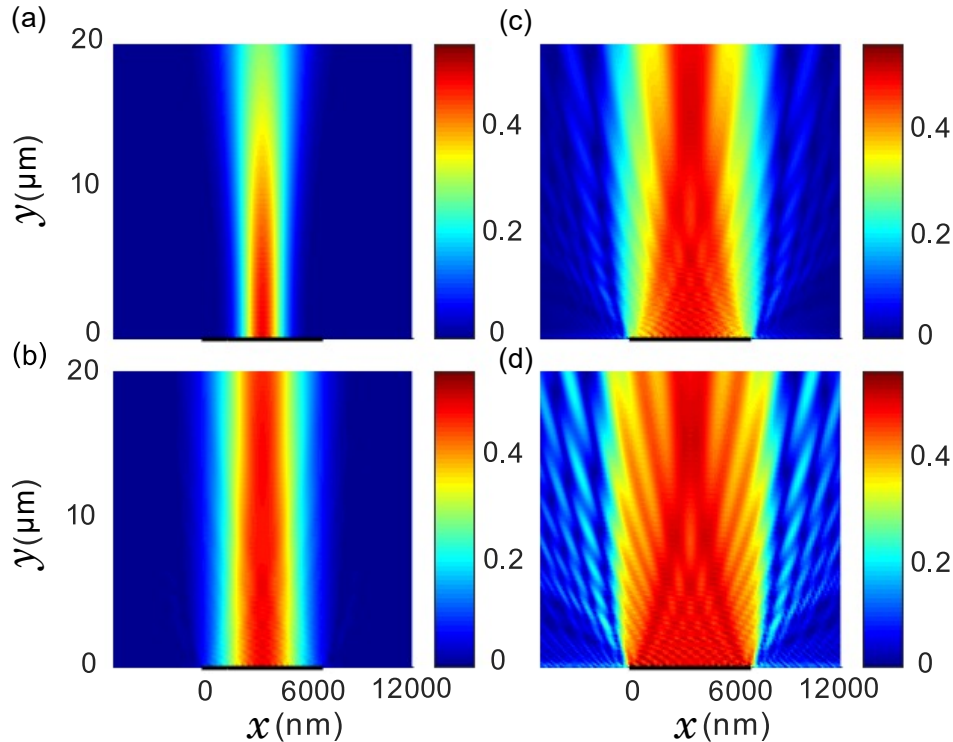

Figure 10. (Color online) Magnitude of time-averaged Poynting vector when a Gaussian beam is incident on a structure consisting of 20 grooves at a wavelength of 660 nm. The horizontal black lines denote the groove array and the ratios are $\gamma = 0.5$ in (a), $\gamma = 1$ in (b), $\gamma = 2$ in (c), and $\gamma = \infty$ (plane wave) in (d).

4. TAPERED GROOVES

Until now rectangular grooves have been examined as illustrated in Fig. 1(a). In this section tapered grooves are considered with a depth of 350 nm, a top width of 100 nm, and a bottom width of 60 nm as seen in Fig. 1(b). In[2] tapered grooves are found to give rise to broader resonances compared to rectangular grooves, which can be understood in terms of the resonator formalism presented therein. The tapered grooves are studied here following the same procedure as for the rectangular grooves studied in Sec. 2 and 3. Thus first two grooves are studied and the cross sections found as a function of distance between the grooves. The result is found to be very similar to Fig. 2 and with approximately the same d giving rise to the extrema. The EXT cross section as a function of wavelength is seen in Fig. 11(a) for a structure consisting of 1, 5, 10, and 20 grooves with $d = 300$ nm between the grooves, where the resonance wavelength is 704 nm. The spectra are quite similar to those of the rectangular grooves in Fig. 5(a) but with a broader resonance. Again the EXT cross section scales almost linear with the number of grooves for the considered wavelengths. The reflectance of the same structure when

illuminating with a Gaussian beam is seen in Fig. 11(b) and follow the same principles as the rectangular grooves in 9(a). Here the beam waist radius w_0 has been fixed at 1925 nm which corresponds to $\gamma = 0.5$ for a structure consisting of 20 grooves. Here the reflectance at resonance is 0.34 even when 20 grooves are present. Hence for the tapered grooves considered here the resonance is broader but it is not possible to achieve perfect absorption as is the case for rectangular grooves.
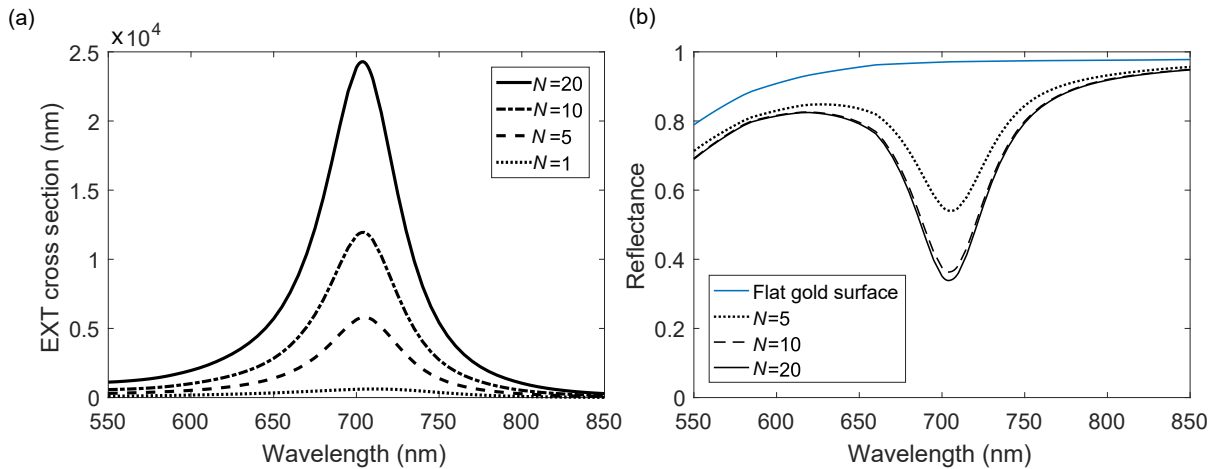

Figure 11. (a) EXT cross section as a function of wavelength for 1, 5, 10, and 20 tapered grooves. (b) Reflectance as a function of wavelength for 5, 10, and 20 tapered grooves. The distance d between the grooves is 300 nm in both (a) and (b).

5. CONCLUSION

The optics of multiple rectangular and tapered grooves in metal have been studied theoretically in order to examine the transition from a single groove to infinitely many grooves arranged in a periodic array. When the incident field is a plane wave the OUP cross section almost depends linearly on the number of grooves, a result that was also recently found for multiple ultrasharp grooves. The OUP cross section per groove is comparable to the groove period even though the scattering structure has a width of many wavelengths. A structure consisting of infinitely many grooves in a periodic array illuminated by a plane wave has a very low reflectance at resonance, but this is not due to destructive interference occurring between the scattered fields of different grooves. Instead a narrow Gaussian beam focused entirely within the grooves has to be used as the incident field in order for the reflectance of multiple grooves to be the same as for an infinite array of grooves illuminated by a plane wave.

When the distance between the rectangular grooves is 300 nm a structure consisting of 20 grooves is found to be a near-perfect absorber for wavelengths close to 657 nm, while it for longer wavelengths is a nearly perfect mirror. When the distance between the grooves increases to 600 nm the reflectance is found to be close to that of pure gold independent on the number of grooves in the structure. For tapered grooves instead the resonance is broader but the minimal reflectance is found to be 0.34 even when 20 grooves are present, and the tapered grooves considered here can therefore not be used a perfect absorber.

Acknowledgement

REFERENCES

[1] Søndergaard, T. and Bozhevolnyi, S. I., "Optics of a single ultrasharp groove in metal," *Opt. Lett.* **41**, 2903–2906 (2016).

[2] Roberts, A., Søndergaard, T., Chirumamilla, M., Pors, A., Beermann, J., Pedersen, K., and Bozhevolnyi., S., "Light extinction and scattering from individual and arrayed high-aspect-ratio trenches in metals," *Phys. Rev. B* **93**, 075413 (2016).

[3] Perchec, J. L., Quémerais, P., Barbara, A., and López-Ríos, T., "Why metallic surfaces with grooves a few nanometers deep and wide may strongly absorb visible light," *Phys. Rev. Lett.* **100**, 066408 (2008).

[4] Pardo, F., Bouchon, P., Haidar, R., and Pelouard, J., "Light funneling mechanism explained by magneto-electric interference," *Phys. Rev. Lett.* **107**, 093902 (2011).

[5] Søndergaard, T., Novikov, S., Holmgaard, T., Eriksen, R., Beermann, J., Han, Z., Pedersen, K., and Bozhevolnyi, S., "Plasmonic black gold by adiabatic nanofocusing and absorption of light in ultra-sharp convex grooves," *Nature Communications* **969**, 1–6 (2012).

[6] Søndergaard, T. and Bozhevolnyi, S. I., "Theoretical analysis of plasmonic black gold: periodic arrays of ultra-sharp grooves," *New J. Phys.* **15**, 013034 (2012).

[7] Skjølstrup, E. J. and Søndergaard, T., "Optics of multiple ultrasharp grooves in metal," *J. Opt. Soc. Am. B* **34**, 673–680 (2017).

[8] Argyropoulos, C., Le, K., Mattiucci, N., Daguanno, G., and Alù, A., "Broadband absorbers and selective emitters based on plasmonic brewster metasurfaces," *Phys. Rev. B* **87**, 205112 (2013).

[9] Skovsen, E., Søndergaard, T., Lemke, C., Holmgaard, T., Leißner, T., Eriksen, R., Beermann, J., Bauer, M., Pedersen, K., and Bozhevolnyi, S., "Plasmonic black gold based broadband polarizers for ultra-short laser pulses," *Appl. Phys. Lett.* **103**, 211102 (2013).

[10] Greffet, J., Carminati, R., Joulain, K., Mulet, J., Mainguy, S., and Chen, Y., "Coherent emission of light by thermal sources," *Nature* **416**, 61–64 (2002).

[11] Miyazaki, H., Ikeda, K., Kasaya, T., Yamamoto, K., Inoue, Y., Fujimura, K., Kanakugi, T., Okada, M., Hatade, K., and Kitagawa, S., "Thermal emission of two-color polarized infrared waves from integrated plasmon cavities," *Appl. Phys. Lett.* **92**, 141114 (2008).

[12] Bauer, T., [*Thermophotovoltaics – Basic Principles and Critical Aspects of System Design*], Springer Verlag Berlin, 1st ed. (2011).

[13] Sai, H. and Yugami, H., "Thermophotovoltaic generation with selective radiators based on tungsten surface gratings," *Appl. Phys. Lett.* **85**, 3399–3401 (2004).

[14] Johnson, P. and Christy, R., "Optical constants of the noble metals," *Phys. Rev. B* **5**, 4370–4379 (1972).

[15] Barrett, R., Berry, M., Chan, T., Demmel, J., Donato, J., Dongarra, J., Eijkhout, V., Pozo, R., Romine, C., and Vorst, H., [*Templates for the Solution of Linear Systems: Building Blocks for Iterative Methods*], SIAM, second ed. (1994).

[16] Mathworks, "gmres." https://se.mathworks.com/help/matlab/ref/gmres.html. (Accessed: 29 June 2017).

[17] Novotny, L. and Hecht, B., [*Principles of Nano-Optics*], Cambridge, second ed. (2012).

[18] Young, H. D., Freedman, R. A., and Ford, A. L., [*University Physics with Modern Physics*], Pearson, 13th ed. (2012).

[19] López-Tejeira, F., García-Vidal, F. J., and Martín-Moreno, L., "Scattering of surface plasmons by one-dimensional periodic nanoindented surfaces," *Phys. Rev. B* **72**, 161405(R) (2005).

[20] Brucoli, G. and Martín-Moreno, L., "Effect of depth on surface plasmon scattering by subwavelength surface defects," *Phys. Rev. B* **83**, 075433 (2011).

[21] Nikitin, A. Y., López-Tejeira, F., and Martín-Moreno, L., "Scattering of surface plasmon polaritons by one-dimensional inhomogeneities," *Phys. Rev. B* **75**, 035129 (2007).

[22] Ropers, C., Neacsu, C. C., Elsaesser, T., Albrecht, M., Raschke, M. B., and Lienau, C., "Grating-coupling of surface plasmons onto metallic tips: A nanoconfined light source," *Nano Lett.* **7**, 2784–2788 (2007).

[23] Radko, I. P., Bozhevolnyi, S. I., Brucoli, G., Martin-Moreno, L., Garcia-Vidal, F., and Boltasseva, A., "Efficiency of local surface plasmon polariton excitation on ridges," *Phys. Rev. B* **78**, 115115 (2008).

[24] Lalanne, P., Hugonin, J., Liu, H., and Wang, B., "A microscopic view of the electromagnetic properties of sub-λ metallic surfaces," *Surface Science Reports* **69**, 453–469 (2009).

[25] Wang, B. and Lalanne, P., "Surface plasmon polaritons locally excited on the ridges of metallic gratings," *J. Opt. Soc. Am. A* **27**, 1432–1441 (2010).

[26] Søndergaard, T., Bozhevolnyi, S. I., Beermann, J., Novikov, S. M., Devaux, E., and Ebbesen, T. W., "Extraordinary optical transmission with tapered slits: effect of higher diffraction and slit resonance orders," *J. Opt. Soc. Am. B* **29**, 130–137 (2012).

[27] Maradudin, A. A., Simonsen, I., Polanco, J., and Fitzgerald, R. M., "Rayleigh and wood anomalies in the diffraction of light from a perfectly conducting reflection grating," *Journal of Optics* **18**, 1–10 (2016).

[28] Fano, U., "The theory of anomalous diffraction gratings," *J. Opt. Soc. Am.* **31**, 213–222 (1941).